0026-895X/09/7603-667–678$20.00
MOLECULAR PHARMACOLOGY
Vol. 76, No. 3
55830/3509858
Mol Pharmacol 76:667–678, 2009
Printed in U.S.A.

Dual Mechanisms of sHA 14-1 in Inducing Cell Death through Endoplasmic Reticulum and Mitochondria

David Hermanson, Sadiya N. Addo, Anna A. Bajer, Jonathan S. Marchant, Sonia Goutam Kumar Das, Balasubramanian Srinivasan, Fawaz Al-Mousa, Francesco Michelangeli, David D. Thomas, Tucker W. LeBien, and Chengguo Xing

Departments of Medicinal Chemistry (D.H., S.N.A., S.G.K.D., B.S., C.X.), Laboratory Medicine and Pathology (A.A.B., T.W.L.), Pharmacology (J.S.M.), Biochemistry, Molecular Biology, and Biophysics (D.D.T.), and the Masonic Cancer Center (T.W.L., C.X.), University of Minnesota, Minneapolis, Minnesota; and School of Biosciences, University of Birmingham, Edgbaston, Birmingham, United Kingdom (F.A., F.M.)

Received February 24, 2009; accepted June 26, 2009

ABSTRACT

HA 14-1 is a small-molecule Bcl-2 antagonist that promotes apoptosis in malignant cells, but its mechanism of action is not well defined. We recently reported that HA 14-1 has a half-life of only 15 min in vitro, which led us to develop a stable analog of HA 14-1 (sHA 14-1). The current study characterizes its mode of action. Because of the antiapoptotic function of Bcl-2 family proteins on the endoplasmic reticulum (ER) and mitochondria, the effect of sHA 14-1 on both organelles was evaluated. sHA 14-1 induced ER calcium release in human leukemic cells within 1 min, followed by induction of the ER stress-inducible transcription factor ATF4. Similar kinetics and stronger intensity of ER calcium release were induced by the sarcoendoplasmic reticulum Ca^{2+}-ATPase (SERCA) inhibitor thapsigargin, accompanied by similar kinetics and intensity of ATF4 induction. sHA 14-1 directly inhibited SERCA enzymatic activity but had no effect on the inositol triphosphate receptor. Evaluation of the mitochondrial pathway showed that sHA 14-1 triggered a loss of mitochondrial transmembrane potential ($\Delta\psi m$) and weak caspase-9 activation, whereas thapsigargin had no effect. (*R*)-4-(3-Dimethylamino-1-phenylsulfanylmethyl-propylamino)-*N*-{4-[4-(4′-chloro-biphenyl-2-ylmethyl)-piperazin-1-yl]-benzoyl}-3-nitrobenzenesulfonamide (ABT-737), a well established small-molecule Bcl-2 antagonist, rapidly induced loss of $\Delta\psi m$ and caspase-9 activation but had no effect on the ER. The pan-caspase inhibitor *N*-benzyloxycarbonyl-Val-Ala-Asp-fluoromethyl ketone had some protective effect on sHA 14-1–induced cell death. These collective results suggest a unique dual targeting mechanism of sHA 14-1 on the apoptotic resistance machinery of tumor cells that includes antiapoptotic Bcl-2 family proteins and SERCA proteins.

Drug resistance is a major challenge in the treatment of cancer. At the molecular level, one major mode of acquiring drug resistance is through the overexpression of antiapoptotic Bcl-2 family proteins (Reed, 2003; Adams and Cory, 2007), which leads to the suppression of apoptosis. Because inducing apoptosis is a key mechanism by which most anticancer drugs eliminate tumor cells, antagonizing antiapoptotic Bcl-2 family proteins is a promising approach in overcoming drug resistance.

Antiapoptotic Bcl-2 family proteins can localize to various organelles, including mitochondria, endoplasmic reticulum (ER), and nucleus (Krajewski et al., 1993; Rong and Distelhorst, 2008). Although the function of nuclear Bcl-2 proteins is uncertain, the functions and mechanisms of these proteins localized to mitochondria and ER in apoptotic regulation are better understood. The mitochondria-localized antiapoptotic

This work was supported by National Institutes of Health National Cancer Institute [Grant R01-CA114294]; the American Association of College of Pharmacy; and the Leukemia Research Fund, Masonic Cancer Center, University of Minnesota.

D.H. and S.N.A. contributed equally to this work and are cofirst authors. T.W.L. and C.X. contributed equally to this work and are cosenior authors.

Article, publication date, and citation information can be found at http://molpharm.aspetjournals.org.
doi:10.1124/mol.109.055830.

ABBREVIATIONS: ER, endoplasmic reticulum; IP_3R, inositol phosphate 3 receptor; SERCA, sarcoendoplasmic reticulum Ca^{2+}-ATPase; HA 14-1, ethyl 2-amino-6-bromo-4-(1-cyano-2-ethoxy-2-oxoethyl)-4*H*-chromene-3-carboxylate; sHA 14-1, ethyl-2-amino-6-phenyl-4-(2-ethoxy-2-oxoethyl)-4*H*-chromene-3-carboxylate; isHA 14-1, ethyl-2-amino-6-phenyl-4-(2-morpholino-2-oxoethyl)-4*H*-chromene-3-carboxylate; ABT-737, (*R*)-4-(3-dimethylamino-1-phenylsulfanylmethyl-propylamino)-*N*-{4-[4-(4′-chloro-biphenyl-2-ylmethyl)-piperazin-1-yl]-benzoyl}-3-nitrobenzenesulfonamide; AM, acetoxymethyl ester; ATF4, activating transcription factor 4; FCCP, carbonylcyanide-4-(trifluoromethoxy)-phenylhydrazone; PIPES, piperazine-*N*,*N*′-bis(2-ethanesulfonic acid); DMSO, dimethyl sulfoxide; SR, sarcoplasmic reticulum; PI, propidium iodide; $\Delta\psi m$, mitochondrial transmembrane potential; TMRE, tetramethylrhodamine; *Z*-VAD-fmk, *N*-benzyloxycarbonyl-Val-Ala-Asp-fluoromethyl ketone; TG, thapsigargin; ROS, reactive oxygen species.

Bcl-2 family proteins antagonize proapoptotic stimuli, prevent mitochondrial depolarization, and suppress the release of proapoptotic molecules critical for apoptosis, such as cytochrome *c* (Ow et al., 2008). The ER-localized antiapoptotic Bcl-2 family proteins suppress apoptosis through regulating calcium homeostasis and preventing sustained cytosolic calcium increases, although the exact mechanism is unsettled (Breckenridge et al., 2003; Xu et al., 2005; Giorgi et al., 2008; Rong and Distelhorst, 2008). Recent studies suggest that ER-localized antiapoptotic Bcl-2 family proteins may regulate calcium homeostasis through modulating ER-localized calcium transporters, including inositol phosphate 3 receptor (IP_3R) (Li et al., 2002; Chen et al., 2004; White et al., 2005; Li et al., 2007; Hanson et al., 2008) and sarcoendoplasmic reticulum Ca^{2+}-ATPase (SERCA) (Kuo et al., 1998; Dremina et al., 2004; Dremina et al., 2006), both of which have been reported to be responsible for drug resistance against certain types of cancer therapies (Denmeade and Isaacs, 2005; O'Neill et al., 2006; Bollig et al., 2007; Lee et al., 2007; Liu et al., 2008).

During the past few years, dozens of small-molecule Bcl-2 protein antagonists have been discovered, and several have entered clinical trials for treatment of hematopoietic malignancies and solid tumors (Letai, 2005; Doshi and Xing, 2008; Reed, 2008). HA 14-1 (Fig. 1) was the first small-molecule Bcl-2 antagonist reported (Wang et al., 2000), and this compound demonstrated selective cytotoxicity against drug-resistant cancer cells that overexpress antiapoptotic Bcl-2 family proteins (Lickliter et al., 2003; Dai et al., 2004). Furthermore, numerous studies have reported synergism of HA 14-1 with cancer therapies of diverse mechanisms of action (Milella et al., 2002, 2004; Nimmanapalli et al., 2003; Pei et al., 2003, 2004; Sinicrope et al., 2004; Sinicrope and Penington, 2005; Manero et al., 2006; Niizuma et al., 2006; An et

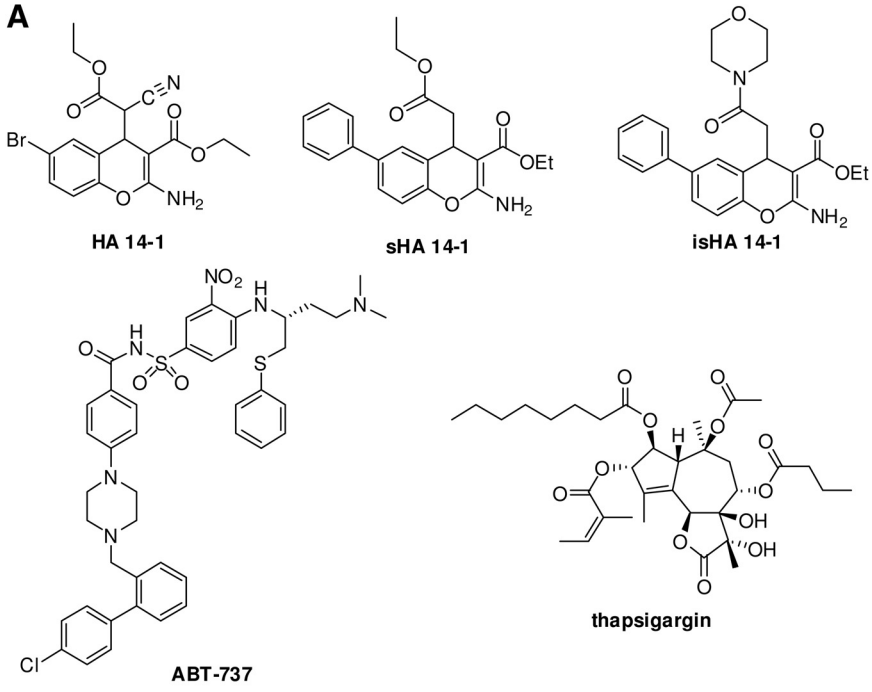

Fig. 1. Structure of the compounds used in the present study and IC_{50} data for sHA 14-1. A, chemical structures of sHA 14-1, isHA 14-1, ABT-737, thapsigargin, and HA 14-1. As described under *Materials and Methods*, isHA 14-1 is an inactive variant of sHA 14-1. B, RS4;11, BLIN-1, and NALM-6 were incubated with various concentrations of sHA 14-1 for 18 h, and Annexin V^-/PI^- viable cells were quantified by flow cytometry. Each condition represents the mean ± S.D. of triplicate values. The results are representative of multiple experiments.

al., 2007; Lickliter et al., 2007), suggesting the potential utility of HA 14-1 in combination therapy for cancer treatment. However, HA 14-1 is highly unstable and rapidly decomposes to inactive species with a half-life of only 15 min in cell culture medium (Doshi et al., 2007). Because of this highly undesirable instability, we synthesized a stable analog of HA 14-1, designated sHA 14-1, that also exhibits synergism and selective toxicity against Bcl-2-overexpressing drug-resistant cancer cells (Tian et al., 2008). The goal of the present study was to elucidate the molecular mechanism of sHA 14-1 in inducing apoptosis. We show that sHA 14-1 has a dual mode of action that involves antagonizing mitochondrial Bcl-2 proteins and inhibits SERCA proteins and induces ER stress.

Materials and Methods

Chemicals and Reagents. The stable analog of HA 14-1, sHA 14-1 (Fig. 1), was synthesized and characterized by NMR and mass spectrometry as described previously (Tian et al., 2008). An inactive variant of sHA 14-1, designated isHA 14-1, was synthesized and characterized following a similar procedure (Fig. 1). isHA 14-1 is different from sHA 14-1 in that the 4′-ethyl is replaced by a morpholinyl group (Fig. 1). ABT-737 (Fig. 1) was synthesized according to published procedures (Oltersdorf et al., 2005). Fura-2AM was from Invitrogen (Carlsbad, CA). Thapsigargin (Fig. 1) was obtained from Acros Organics (Geel, Belgium). EGTA-AM was from VWR Scientific (Batavia, IL). Carbonylcyanide-4-(trifluoromethoxy)-phenylhydrazone (FCCP) and probenecid were from Sigma-Aldrich (St Louis, MO). $^{45}Ca^{2+}$ (27 mCi/ml) was from PerkinElmer Life and Analytical Sciences (Waltham, MA). CellTiter Blue Assay Kit was from Promega (Madison, WI). The anti-activating transcription factor-4 (ATF4) antibody was from Santa Cruz Biotechnology, Inc. (Santa Cruz, CA) and was used at a final dilution of 1:500. The anti-Bcl-2 antibody was from Sigma-Aldrich and was used at a final dilution of 1:1000. The anti-caspase-9 antibody was from Cell Signaling Technology (Danvers, MA) and was used at a final dilution of 1:1000.

Cell Culture and Treatment. JURKAT and U937 human leukemic cell lines were obtained from the American Type Culture Collection (Manassas, VA). The human B-lineage acute lymphoblastic leukemia cell lines BLIN-1 (Wörmann et al., 1989), RS4;11 (Stong et al., 1985), and NALM-6 (Hurwitz et al., 1979) were either originally established or originally characterized at the University of Minnesota. All human leukemic cell lines were maintained in RPMI-1640 medium + L-glutamine supplemented with 10% fetal bovine serum and 1% penicillin/streptomycin. The chicken DT-40 B lymphoma cell line and IP_3R-null DT-40 cell line (Sugawara et al., 1997) were kindly provided by Dr. Chi Li (University of Louisville, Louisville, KY). Both DT-40 cell lines were cultured in RPMI-1640 medium + L-glutamine supplemented with 10% fetal bovine serum, 1% chicken serum, and 1% penicillin/streptomycin. All cell lines were incubated at 37°C with 5% CO_2 in air atmosphere.

Evaluation of Cell Viability. Leukemic cells were plated at a density of 10^4 cells/well in a 96-well round-bottomed plate. Test compounds were added at varying concentrations in 1% DMSO, and cells were treated with medium containing 1% DMSO served as a control. After a 24-h treatment, relative cell viability in each well was determined using the CellTiter-Blue Cell Viability Assay. The IC_{50} of each compound was determined by fitting the relative viability of the cells to the drug concentration, using a dose-response model in Prism software (GraphPad Software, San Diego, CA).

Determination of Cytosolic Calcium Concentration. Cells at a density of 10^6 cells/ml were incubated in medium containing 5 μM Fura-2AM and 2.5 mM probenecid at room temperature in the dark for 30 min. The cells were then washed once with ice-cold phosphate-buffered saline and re-suspended to a concentration of 2×10^6 cells/ml in medium containing 2.5 mM probenecid. To a cuvette with 735 μl of media containing 100 mM EGTA and 2.5 mM probenecid was added 750 μl of the cell suspension. The cell suspension was mixed by a slow stirring magnetic bar. Under these conditions, the cell medium contained a negligible amount of free calcium. Therefore, the cells had no extracellular calcium source. Fluorescence emission was measured for 1 min followed by addition of 15 μl of medium containing sHA14-1, and readings were continued for another 9 min. Readings were obtained on a dual-wavelength fluorometer (Cary Eclipse; Varian, Palo Alto, CA) with excitation wavelengths alternating between 340 and 380 nm and an emission wavelength of 510 nm.

The effelct of sHA 14-1 on Thapsigargin-Induced ER Calcium Release. This experiment followed the same procedures as those described under *Determination of Cytosolic Calcium Concentration*, except that extracellular calcium was not chelated by EGTA in this assay.

$^{45}Ca^{2+}$ Assays. NALM-6 cells (10^8cells/ml) were suspended in 25 ml of calcium-free medium (140 mM KCl, 20 mM NaCl, 2 mM $MgCl_2$, 1 mM EGTA, and 20 mM PIPES, pH 7 at 37°C). The cells were incubated in a gyratory waterbath and permeabilized by adding 5-μl increments of 10 μg/ml saponin, and membrane permeability was monitored by trypan blue staining. Permeabilized cells were centrifuged and resuspended in 6 ml of cytosol-like medium [140 mM KCl, 20 mM NaCl, 2 mM $MgCl_2$, 1 mM EGTA, 300 μM $CaCl_2$ (free [Ca^{2+}], ~200 nM), and 20 mM PIPES, pH 7 at 37°C]. For loading experiments, cells were separated into two tubes, one containing DMSO and the other containing sHA 14-1 (50 μM), and were then incubated with $^{45}Ca^{2+}$ (~5 μCi/ml) in the presence of FCCP (10 μM). A cell sample containing 10 μM thapsigargin (TG) was used as the background control. At appropriate times, 200-μl aliquots were transferred to separate tubes with the addition of 5 mM ATP. Incubations were terminated by filtration over GF/C filters, washed with sucrose/citrate solution [310 mM sucrose, 1 mM trisodium citrate]. The filter discs were collected, soaked in scintillation liquid overnight, and the radioactive counts were quantified the following day. Ca^{2+} uptake was then plotted in the absence and presence of sHA 14-1 with the use of GraphPad Prism 4; thapsigargin-treated samples were used as the background radioactive counts. For Ca^{2+} release assays, NALM-6 or U937 cells (10^8 cells/ml) were permeabilized as described above and resuspended in 6 ml of cytosol-like medium containing 10 μM FCCP, 5 mM ATP, and 6 μl of $^{45}Ca^{2+}$. After loading to steady state (~10 min), samples (200 μl) were transferred into tubes containing different concentrations of either IP_3 or sHA 14-1. After a 5-min incubation, the cells were filtered over GF/C filter paper and processed as described above.

Measurement of SERCA Enzymatic Activity. Rabbit skeletal muscle sarcoplasmic reticulum (SR) Ca^{2+} ATPase was used as a source of SERCA 1A, and enzymatic activity was measured using a coupled enzymatic assay as described previously (Michelangeli and Munkonge, 1991). Pig brain microsome Ca^{2+} ATPase (Bilmen and Michelangeli, 2002) was used as a source of SERCA2B, and enzymatic activity was measured using a phosphate liberation assay as described previously (Wootton and Michelangeli, 2006). To prepare highly purified SERCA samples, SR vesicles prepared from fast-twitch skeletal muscle of New Zealand White rabbits (Fernandez et al., 1980) was purified on a discontinuous sucrose gradient (Birmachu et al., 1989) to remove junction SR-containing calcium release channels. The resulting SR was further purified on a reactive red column to produce a preparation in which at least 99% of the protein was SERCA (Reddy et al., 2003).

Flow Cytometric Detection of Apoptotic Cells, Mitochondrial Membrane Depolarization, and Cytochrome *c* Release. Apoptotic cells were detected by staining with Annexin V and propidium iodide (PI). The loss of mitochondrial transmembrane potential ($\Delta\psi m$) was detected by staining cells with the cationic lipophilic fluorescent dye tetramethylrhodamine (TMRE), using a FACSCalibur (BD Biosciences, San Jose, CA). Detection of cytochrome *c* was

accomplished using the Innocyte Flow Cytometric Cytochrome *c* Release Kit (Calbiochem, San Diego, CA) according to the manufacturer's instructions. All procedures were conducted as described previously (Shah et al., 2004).

Western Blotting. Western blotting was conducted using standard chemiluminescent techniques as described previously (Shah et al., 2004). After a 2- to 4-h incubation in primary antibody at room temperature, the blot was washed, and secondary staining was accomplished using the corresponding IgG conjugated to horseradish perioxidase. Protein loading was assessed using anti-β-tubulin or anti-AKT.

Statistics. All biological experiments, including in vitro cytotoxicity assays and calcium assays, were performed at least three times. Flow cytometry and Western Blot analyses are representative of many experiments. Data are presented as means ± S.D., and comparisons were made using Student's *t* test. A probability of 0.05 or less was considered statistically significant.

Results

Characterization of Apoptotic Induction by sHA 14-1 and isHA 14-1. Before conducting studies on the mechanism of action of sHA 14-1, we examined its capacity to induce apoptosis in several widely used B-lineage acute lymphoblastic leukemia cell lines. Overnight incubation with sHA 14-1 (6–100 μM) showed that NALM-6, BLIN-1, and RS4;11 had similar sensitivities, with an IC_{50} of ~50 μM (Fig. 1B). It is noteworthy that the inactive variant isHA 14-1 had absolutely no proapoptotic effect when tested between 6 and 100 μM for up to 24 h (data not shown).

Effect of sHA 14-1 on Cellular Ca^{2+} Homeostasis. Although ER-localized antiapoptotic Bcl-2 family proteins have been demonstrated to inhibit apoptosis by modulating ER calcium storage and release (Kuo et al., 1998; Pinton and Rizzuto, 2006; Giorgi et al., 2008), the effect of Bcl-2 antagonists on intracellular calcium regulation has been minimally studied (An et al., 2004). Analysis of human leukemia cells revealed that sHA 14-1 induced a dose-dependent release of calcium in NALM-6 (Fig. 2A) and JURKAT (Fig. 2B). The well studied SERCA inhibitor thapsigargin rapidly increased cytosolic calcium through the release of ER calcium in NALM-6 (Fig. 2C) and JURKAT (Fig. 2D). The kinetics of

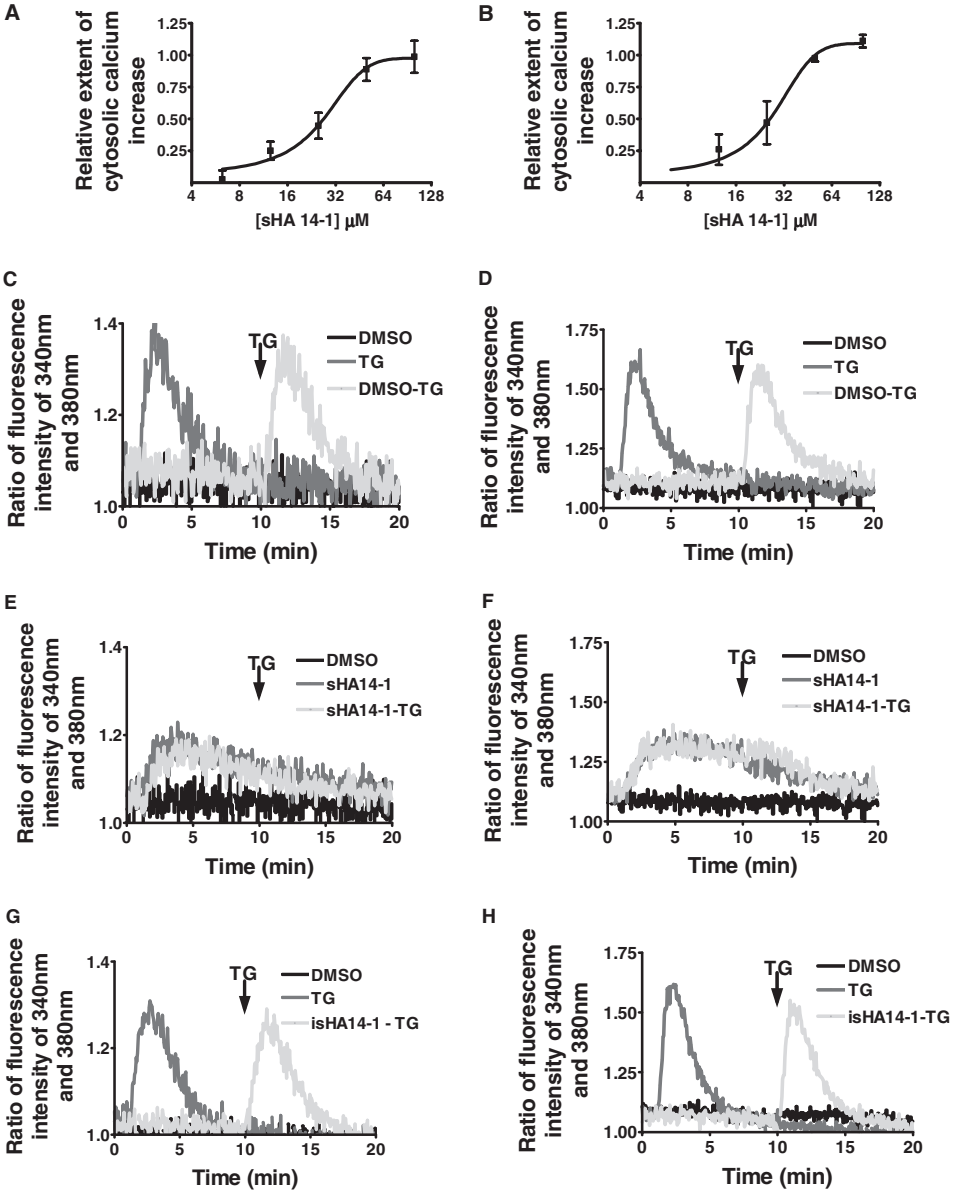

Fig. 2. sHA 14-1 induces ER calcium release. NALM-6 (A, C, E, and G) and JURKAT (B, D, F, and H) were preloaded with Fura-2AM for 30 min. The cells were then washed, and fluorescent changes at excitation wavelengths of 340 and 380 nm were monitored on a dual-wavelength fluorometer. Data in A and B show the relative extent of cytosolic [Ca^{2+}] changes after a 10-min incubation with the indicated concentrations of sHA 14-1 (normalized to the maximum cytosolic [Ca^{2+}] increase induced by sHA 14-1 treatment). Data are mean ± S.D. (n = 3 for each conditions). Data in C to H show real-time changes in cytosolic [Ca^{2+}] in cells treated with DMSO, 1 μM thapsigargin, 100 μM sHA 14-1, or 100 μM isHA 14-1. The gray tracings indicate that thapsigargin was added 10 min after the initial addition of DMSO (C and D), sHA 14-1 (E and F), or isHA 14-1 (G and H). The results are representative of three separate experiments.

increased cytosolic calcium induced by sHA 14-1 was similar to that induced by thapsigargin (Fig. 2, E and F). Furthermore, addition of thapsigargin after sHA 14-1 resulted in no significant cytosolic calcium increase beyond that induced by sHA 14-1 alone (Fig. 2, E and F). This lack of additivity implied that both compounds were emptying the same pool of intracellular Ca^{2+}: namely the ER calcium store. isHA 14-1, the inactive analog of sHA 14-1, induced no cytosolic calcium increase (Fig. 2, G and H). The well known Bcl-2 antagonist ABT-737 did not induce significant ER calcium release under the same experimental conditions (data not shown).

Because cytosolic calcium can mediate apoptosis (Szalai et al., 1999; Pinton et al., 2001), and because ER-localized Bcl-2 proteins inhibit apoptosis through control of ER calcium release (Scorrano et al., 2003; Thomenius and Distelhorst, 2003; Zong et al., 2003), the cytotoxic effect of sHA 14-1 might be mediated by ER calcium release. To test this possibility, NALM-6 cells were pretreated with EGTA-AM, a cell-permeable ester form of EGTA that chelated cytosolic calcium induced by sHA 14-1. Evaluation of cytotoxicity demonstrated that EGTA-AM pretreatment decreased the cytotoxicity of sHA 14-1 to NALM-6 (Fig. 3A). Considering that EGTA is good for short-term buffering of calcium, it is not surprising that the protective effects of EGTA were small; nevertheless, these results suggest that ER-released calcium is at least partially responsible for the cytotoxicity induced by sHA 14-1.

Targeting the ER to Induce Calcium Release. To determine whether sHA 14-1 directly interacts with ER to induce Ca^{2+} release, we examined $^{45}Ca^{2+}$ fluxes in permeabilized NALM-6 cells. These experiments were conducted in the presence of FCCP, a mitochondrial uncoupler (Hutson et al., 1976), to prevent Ca^{2+} uptake into mitochondria. In cells pretreated with sHA 14-1, the extent of ER-localized $^{45}Ca^{2+}$ accumulation was lower than that in control cells (Fig. 3B). Furthermore, in cells loaded to steady state with $^{45}Ca^{2+}$,

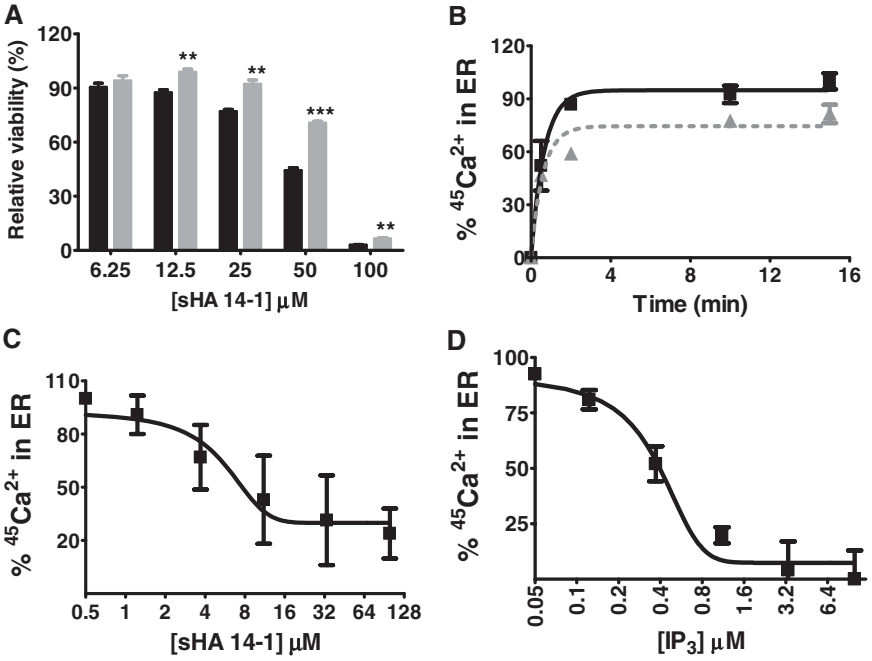

Fig. 3. Cytosolic $[Ca^{2+}]$ is an essential factor for sHA 14-1-induced cytotoxicity and sHA 14-1 directly targets the ER. A, untreated NALM-6 cells (black solid bar) or cells pretreated for 30 min with 5 μM EGTA-AM (gray bar) were incubated with the indicated concentrations of sHA 14-1. Relative cell viability was determined at 24 h by the Cell Titer-Blue cytotoxicity assay. Data are mean ± S.D. (n = 3 for each condition). Results are representative of three separate experiments. **, $p < 0.01$; ***, $p < 0.0001$. B, time course of Ca^{2+} uptake into intracellular Ca^{2+} stores in control cells (■) and cells pretreated (5 min) with sHA 14-1 (50 μM, △). Data are expressed relative to the final time point intracellular Ca^{2+} content. C and D, Ca^{2+} release from permeabilized NALM-6 cells loaded to steady state with $^{45}Ca^{2+}$ induced by various concentrations of sHA 14-1 (C) or IP_3 (D). Data are expressed relative to the zero time point before addition of ATP. Data are mean ± S.D. (n = 3 for each conditions). The results are representative of two separate experiments.

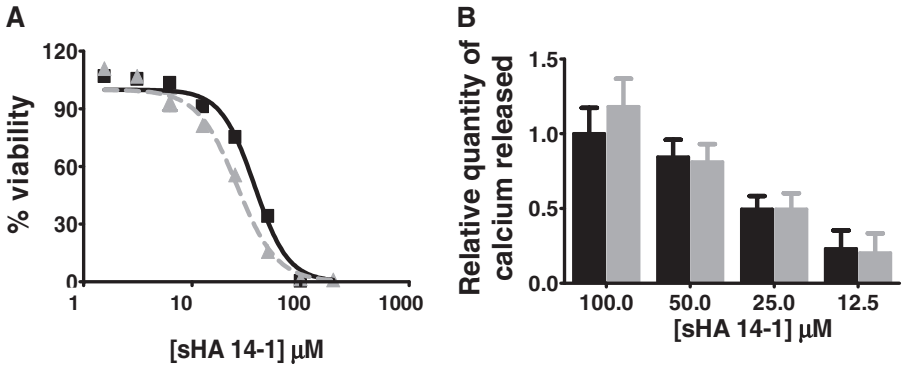

Fig. 4. sHA 14-1 does not disrupt the function of the endoplasmic reticulum IP_3R. A, parental (black bar) and IP_3R-deficient (gray bar) DT-40 chicken lymphoma cells were incubated with the indicated concentrations of sHA 14-1, and relative cell viability was determined after 24 h by the Cell TiterBlue cytotoxicity assay. B, parental (black column) and IP_3R-deficient (gray column) DT-40 chicken lymphoma cells were preloaded with Fura-2AM and treated with sHA 14-1 at indicated concentrations. Relative calcium release was measured using fluorescent changes at excitation wavelengths of 340 and 380 nm monitored on a dual-wavelength fluorometer and normalized to the amount of calcium release by thapsigarin in parental cells at the concentration of 1 μM. Data are mean ± S.D. (n = 3 for each conditions). None of the difference in calcium release in parental and IP_3R-deficient cells is statistically significant ($P > 0.05$). The results are representative of three separate experiments.

2-min sHA 14-1 treatment resulted in a loss of ER Ca^{2+} in a dose-dependent manner (EC_{50} of 4.1 μM; Fig. 3C). As a control, IP_3 effected a more potent depletion (EC_{50} of 106 nM; Fig. 3D). Similar results were obtained using U937 cells (data not shown). Therefore, both experiments implied that sHA 14-1 caused a dose-dependent loss of Ca^{2+} from the ER via directly targeting ER-localized biomolecule(s).

Inhibition of SERCAs by sHA 14-1. Because IP_3Rs and SERCAs are two major ER-localized calcium regulatory transporters that interact with ER-localized Bcl-2 family proteins to regulate cellular calcium homeostasis (Kuo et al., 1998; Li et al., 2002, 2007; Chen et al., 2004; Dremina et al., 2004, 2006; Oakes et al., 2005; White et al., 2005; Hanson et al., 2008), sHA 14-1 may induce ER calcium release by modulating either or both of these targets. To determine whether perturbation of the IP_3Rs was responsible for sHA 14-1–induced ER calcium release, we tested the effect of sHA 14-1 on IP_3R-null DT-40 cells and DT-40 parent cells. These two cell lines were evaluated for their sensitivity to sHA 14-1 based on cytotoxicity and extent of calcium release. As shown

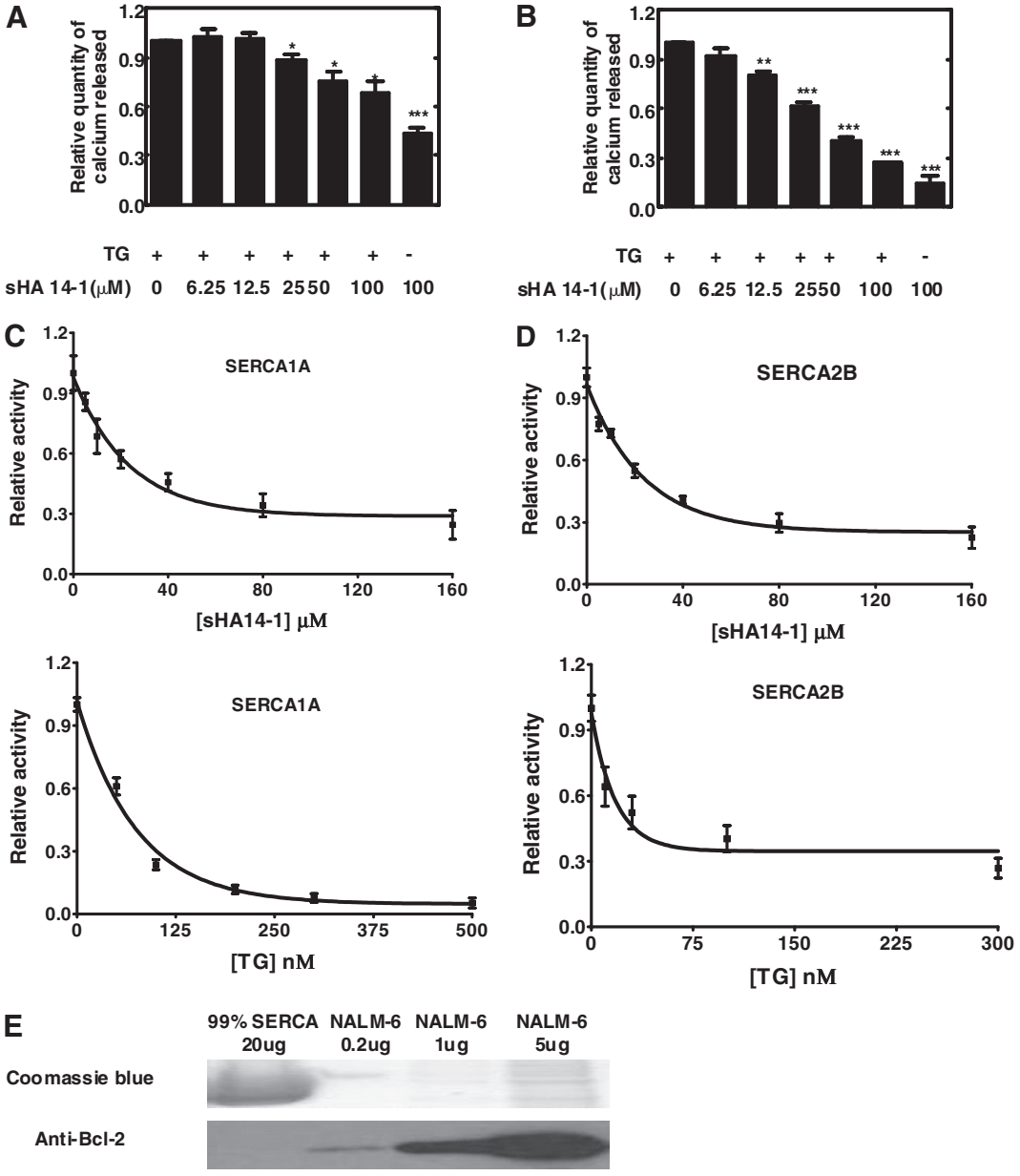

Fig. 5. sHA 14-1 inhibits SERCA enzymatic activity. NALM-6 (A) and JURKAT (B) cells were preloaded with Fura-2AM for 30 min. The cells were then incubated with 100 nM thapsigargin (+), the minimal concentration to induce full Ca^{2+} release, and increasing concentrations of sHA 14-1, as shown in the grid below the figures. Calcium release was quantified using fluorescent changes at excitation wavelengths of 340 and 380 nm monitored on a dual-wavelength fluorometer. Data are mean ± S.D. ($n = 3$ for each conditions). *, $p < 0.05$; **, $p < 0.01$; ***, $p < 0.0001$ compared with the quantity of calcium released by TG alone. C, increasing concentrations of sHA 14-1 were incubated for 10 min at 37°C with SR membrane fractions purified from rabbit skeletal muscle. Rabbit skeletal muscle Ca^{2+} ATPase activity (corresponding to SERCA 1A) was measured using the phosphate liberation assay, as described previously (Wootton and Michelangeli, 2006). Data are mean ± S.D. ($n = 3$ for each conditions). D, increasing concentrations of sHA 14-1 were incubated for 10 min at 37°C with pig brain microsomes. Ca^{2+} ATPase activity in these membranes (corresponding to SERCA 2B) was measured using a phosphate liberation assay, as described previously. Data are mean ± S.D. ($n = 3$ for each conditions). E, a SERCA sample (99%, 20 μg) was analyzed for the presence of Bcl-2 protein by Western blot with NALM-6 protein lysate (0.2, 1, and 5 μg) as a positive control. The results are representative of three separate experiments.

in Fig. 4A, sHA 14-1 demonstrated similar cytotoxicity in both cell lines, with the IP_3R-null line being slightly more sensitive (IP_3R-null DT-40 was found to be moderately more sensitive to other standard anticancer agents as well; data not shown). Figure 4B shows that sHA 14-1 induced the same degree of calcium release in both cell lines. Together, these data suggest that IP_3Rs are unlikely to be the molecular targets responsible for sHA 14-1–induced ER calcium release.

We then explored whether SERCAs might be a target responsible for sHA 14-1–induced ER calcium release. We first tested whether sHA 14-1 may interfere with thapsigargin in ER-calcium release. NALM-6 and JURKAT leukemic cells were cotreated with 100 nM thapsigargin, the minimal concentration to induce full Ca^{2+} release, and increasing concentrations of sHA 14-1. sHA 14-1 indeed antagonized thapsigargin-induced calcium release in a dose-dependent manner (Fig. 5, A and B), suggesting that sHA 14-1 may compete with thapsigargin to interact with SERCAs. We next examined the effect of sHA 14-1 on SERCA enzymatic activity using SR membranes purified from rabbit skeletal muscle for SERCA 1A (Fig. 5C) and from pig brain for SERCA 2B (Fig. 5D). The results show that sHA 14-1 demonstrated moderate inhibition of SERCA 1A and 2B with IC_{50} values of 29.2 ± 4.9 and 23.5 ± 4.2 μM, respectively. Finally, because SERCA has been reported to be regulated by Bcl-2 (Kuo et al., 1998; Dremina et al., 2004, 2006), we considered it possible that sHA 14-1 might modulate SERCA function through antagonizing Bcl-2 protein. Because only 75% of the proteins from the samples used in Fig. 5, A to D, were SERCAs, we prepared samples in which >99% proteins were SERCAs, and sHA 14-1 demonstrated similar inhibitory activity (data not shown). Figure 5E shows a Coomassie Blue stain and Western blot of this 99%-purified SERCA sample, which detected no Bcl-2 proteins (no Bcl-X_L or MCL-1 proteins as well, based on Western analyses; data not shown). As a control, we electrophoresed decreasing concentrations of NALM-6 total protein lysate, and Bcl-2 was easily detected when as little as 0.2 μg of protein was blotted (Fig. 5E). These results suggest that SERCAs are likely to be directly antagonized by sHA 14-1, resulting in an increase in cytosolic calcium and depletion of ER calcium storage.

sHA 14-1 Induced ER and Mitochondrial Stress. Given the effect of sHA 14-1 on ER calcium release (Fig. 2), we next examined whether it would induce ER stress. Expression of the ER stress-associated transcription factor ATF4/CREB-2, one of the characteristics of an ER stress response, was therefore evaluated by Western blotting. Exposure of NALM-6 to 50 μM sHA 14-1 led to induction of ATF4 between 30 and 60 min (Fig. 6A), and a dose response analysis indicated increasing induction from 25 to 100 μM sHA 14-1 (Fig. 6B). Incubation of NALM-6 with thapsigargin served as a positive control. To compare the mechanism of action of sHA 14-1 with that of ABT-737, we used the RS4;11 human leukemic cell line, which has been shown previously to be highly sensitive to ABT-737 (Del Gaizo Moore et al., 2008). As shown in Fig. 6C, ATF4 was induced by sHA 14-1 but not ABT-737. Thapsigargin served as a positive control and isHA 14-1 served as a negative control for ATF4 induction (Fig. 6C).

The effects of sHA 14-1 on $\Delta\psi$m and cytochrome *c* release were evaluated by flow cytometry. Preliminary experiments revealed that loss of $\Delta\psi$m was not detected until 6 h after addition of sHA 14-1 to NALM-6 (data not shown). As shown in Fig. 7A, exposure of NALM-6 to 50 and 100 μM sHA 14-1 for 8 h induced a loss of $\Delta\psi$m based on reduction in TMRE staining intensity. Cells treated with identical concentrations of the inactive variant isHA 14-1 did not undergo changes in $\Delta\psi$m. ABT-737 also induced a loss of $\Delta\psi$m (Fig. 7A) that was detectable as early as 2 h (data not shown). As expected based on its well characterized mechanism of action as a BH3 mimetic (Oltersdorf et al., 2005; Del Gaizo Moore et al., 2008), ABT-737 rapidly induced cytochrome *c* release. However, incubation of NALM-6 for 8 h with sHA 14-1 did not induce detectable cytochrome *c* release (Fig. 7A). The different effects of sHA 14-1 and ABT-737 on cytochrome *c*

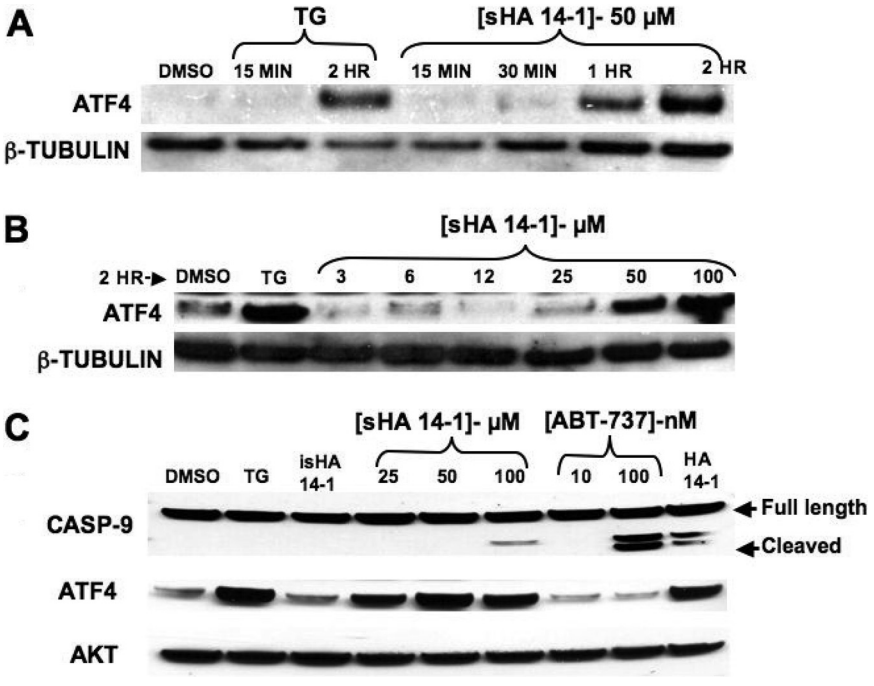

Fig. 6. sHA 14-1 induces ER stress. NALM-6 cells were incubated with 1 μM TG or 50 μM sHA 14-1 for the indicated times (A) or with 1 μM thapsigargin and the indicated concentrations of sHA 14-1 for 2 h (B). RS4;11 cells were incubated with the indicated compounds and concentrations for 2 h (C). DMSO (2 h) was used as a negative control. The cells were then lysed and Western-blotted for detection of ATF4 and cleaved caspase-9 (Casp-9) as described under *Materials and Methods*. β-Tubulin (A and B), or AKT (C) were used as loading controls. The results are representative of three separate experiments.

release was not unique to NALM-6, because analysis of RS4;11 yielded comparable results (Fig. 7B). The failure of sHA 14-1 to induce a loss of cytochrome *c* could not be explained by kinetics, because analysis at earlier (2–4 h) and later (10–14 h) time points gave the same results (data not shown).

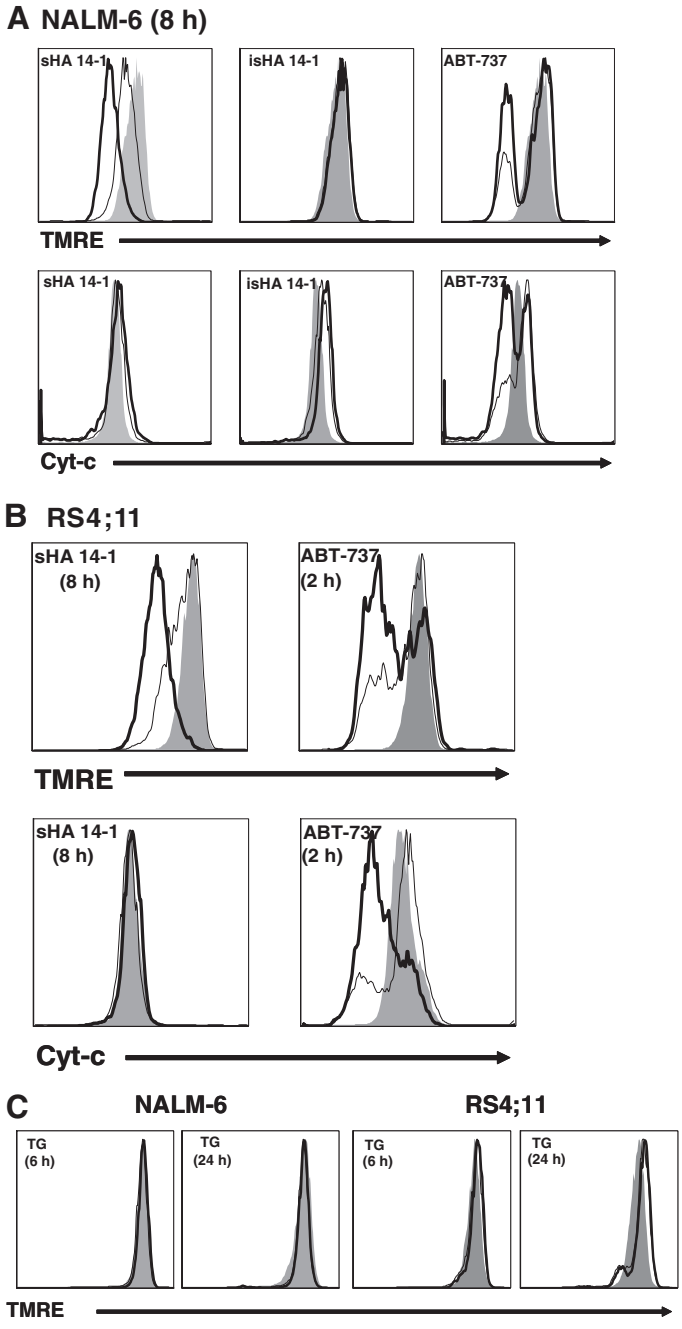

Fig. 7. sHA 14-1 induces loss of $\Delta\psi$m but no detectable cytochrome *c* release by flow cytometry. A, NALM-6 cells were incubated with sHA 14-1 or isHA 14-1 at 50 μM (dashed line) or 100 μM (solid line) or ABT-737 at 5 μM (dashed line) or 10 μM (solid line) for 8 h. B, RS4;11 cells were incubated for 8 h with 50 μM (dashed line) or 100 μM (solid line) sHA 14-1 or for 2 h with 0.3 μM (dashed line) or 1 μM (solid line) ABT-737. C, NALM-6 and RS4;11 cells were incubated with 0.1 μM (dashed line) or 1 μM (solid line) thapsigargin for 6 or 24 h. Cells were stained with TMRE or anti-cytochrome *c* and analyzed by flow cytometry. The gray-shaded histograms show TMRE staining intensity or cytochrome *c* detection in untreated cells. Results are representative of three separate experiments.

Because thapsigargin and sHA 14-1 exerted similar effects on ER calcium release (Fig. 2) and ER stress (Fig. 6), we assessed whether thapsigargin would induce a loss of $\Delta\psi$m similar to that induced by sHA 14-1. The results in Fig. 7C show that 0.1 and 1 μM thapsigargin had no effect on $\Delta\psi$m after 6-h incubation with NALM-6 or RS4;11 and only a very subtle effect on RS4;11 ($< 10\%$ of cells) at 24 h. Other experiments tested thapsigargin at concentrations ranging from 0.1 nM to 1 μM for 2 to 48 h. At no time and at no concentration did we detect a reduction in $\Delta\psi$m similar to that exerted by sHA 14-1 and ABT-737 (data not shown). Thus, despite their similar capacity to induce ER calcium release and ATF4, sHA 14-1 and thapsigargin exert different effects on $\Delta\psi$m.

Although we could not detect sHA 14-1-induced cytochrome *c* release by flow cytometry (Fig. 7A), this may have been the result of assay sensitivity (Tian et al., 2008). We therefore assessed caspase-9 activation as a surrogate outcome of mitochondrial damage and cytochrome *c* release. Figure 6C shows that incubation of RS4;11 with sHA 14-1 for 2 h resulted in a detectable caspase-9 cleavage product at 100 μM. In contrast, thapsigargin and isHA 14-1 did not induce cleavage of caspase-9. As expected, ABT-737 induced robust cleavage of caspase-9, as did HA 14-1. These collective results suggest a primary targeting effect of ABT-737 and thapsigargin on the mitochondria and ER, respectively, and a dual mode of action of sHA 14-1.

Given the minimal effect of sHA 14-1 on loss of mitochondrial cytochrome *c* (Fig. 7) and activation of caspase-9 (Fig. 6C), we assessed the relative degree of caspase dependence using the pan-caspase inhibitor *Z*-VAD-fmk. RS4;11 cells were incubated overnight with sHA 14-1 in the absence or presence of *Z*-VAD-fmk, and cell survival/apoptosis was assessed by PI/Annexin V staining. The results show that incubation with DMSO, the inactive compound isHA 14-1, *Z*-VAD-fmk by itself, or TG had no effect on RS4;11 cells based on light scatter characteristics and PI/Annexin V staining (Fig. 8). Incubation with ABT-737 gave the expected increase in Annexin V^+/PI^- and Annexin V^+/PI^+ events compared with the DMSO control. Also evident is that the majority of ABT-737-treated cells underwent a uniform decrease in cell size, as shown by a decrease in forward light scatter characteristics (Fig. 8; note events circled by dashed line). This is the prototypical change that occurs in cells undergoing apoptosis through the mitochondrial pathway. As expected, inclusion of *Z*-VAD-fmk reduced the frequency of Annexin V^+/PI^- events in ABT-737-treated cells from 31 to 11%, and a concomitant increase (18 to 66%) in cells with viable light scatter characteristics. In contrast, inclusion of *Z*-VAD-fmk in sHA 14-1–treated cells had no effect on the percentage of Annexin V^+/PI^- events and a modest effect on the percent-

Fig. 8. sHA 14-1–induced cell death is largely caspase-independent. RS4;11 cells were incubated with DMSO, 50 μM *Z*-VAD-fmk alone, 100 μM isHA 14-1, 1 μM TG, 100 μM sHA 14-1, 100 μM sHA 14-1 + 50 μM *Z*-VAD-fmk, 100 nM ABT-737, or 100 nM ABT-737 + 50 μM *Z*-VAD-fmk. After 18 h, cells were stained with PI and Annexin V. The data are shown as the light-scatter characteristics on the left side of each condition tested and the PI/Annexin V (ANV) staining as contour plots on the right side of each condition tested. PI/Annexin V analysis was conducted on the cells outlined by the solid line in the light scatter dot plots. The events within the dashed circles in the sHA 14-1– and ABT-737-treated cells are shown to distinguish the difference in light scatter characteristics between the two treated populations. FSC, forward scatter; SSC, side scatter.

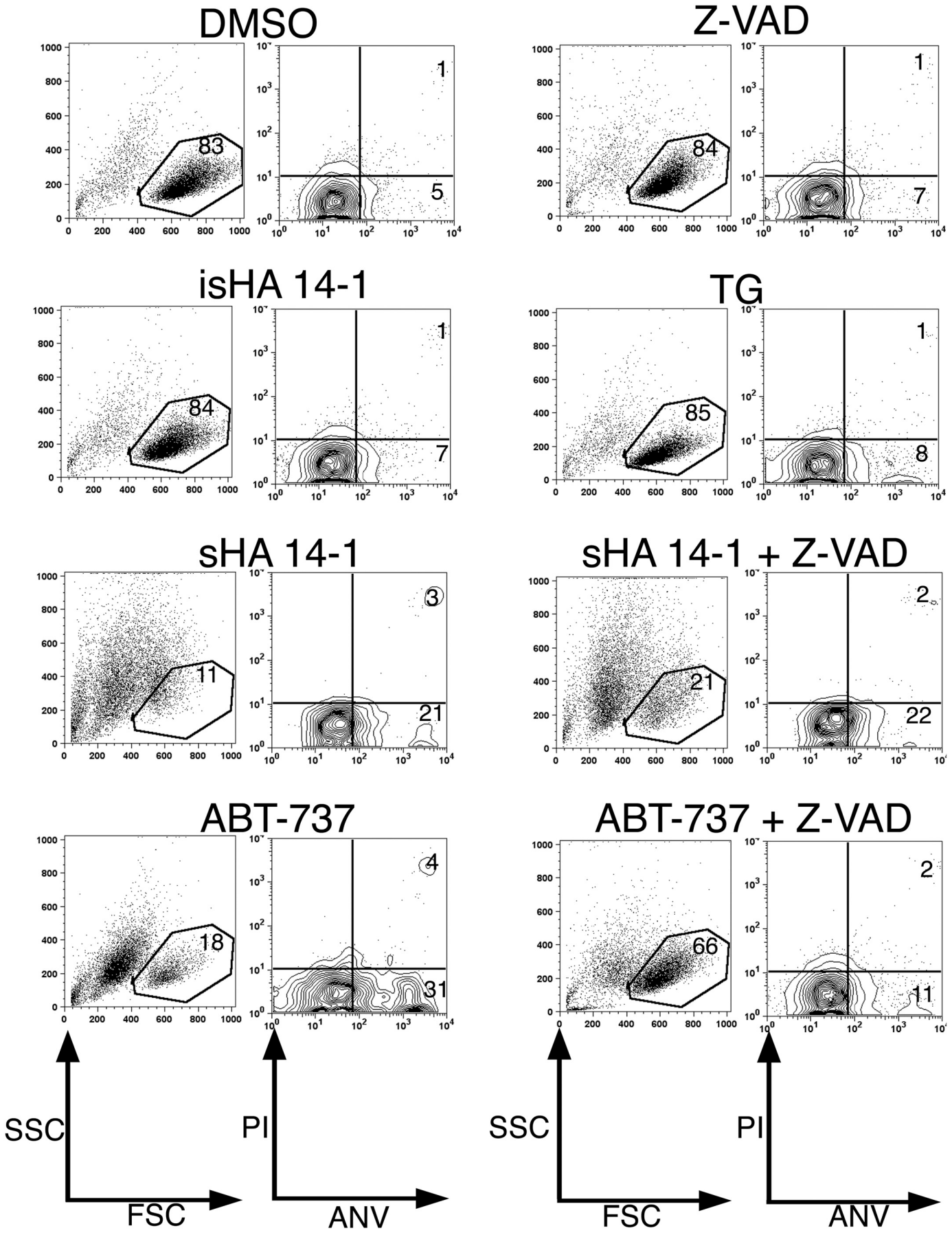
DMSO
83
1
5
Z-VAD
84
1
7
isHA 14-1
84
1
7
TG
85
1
8
sHA 14-1
11
3
21
sHA 14-1 + Z-VAD
21
2
22
ABT-737
18
4
31
ABT-737 + Z-VAD
66
2
11
SSC
FSC
PI
ANV
SSC
FSC
PI
ANV

Fig. 8.

age of cells with viable light scatter characteristics (11 to 21%). Of note is the profound difference in the overall light scatter characteristics of sHA 14-1– and ABT-737-treated cells, the former exhibiting a much greater degree of side-scatter heterogeneity than the latter.

Discussion

Rational drug design that targets antiapoptotic Bcl-2 family members is a promising approach to treating cancer (Letai, 2008). Despite the proven efficacy of compromising Bcl-2 function and unleashing the proapoptotic activity of BAX/BAK and BH-3-only proteins, the intracellular events that culminate in the demise of tumor cells may differ depending on the antagonist. HA 14-1 is an organic compound originally discovered by computer modeling that predicted binding to Bcl-2 (Wang et al., 2000). It has been reported to synergize with a variety of anticancer agents to promote apoptosis in hematopoietic and solid tumors (Milella et al., 2002, 2004; Nimmanapalli et al., 2003; Pei et al., 2003, 2004; Sinicrope et al., 2004; Sinicrope and Penington, 2005; Manero et al., 2006; Niizuma et al., 2006; An et al., 2007; Lickliter et al., 2007). However, we have demonstrated previously that HA 14-1 is highly unstable when incubated in standard tissue culture conditions and has a half-life of ~15 min (Doshi et al., 2007). Of additional concern was the observation that HA 14-1 decomposes to generate reactive oxygen species (ROS), which have potent proapoptotic activity (Doshi et al., 2007). Thus, many prior published studies of HA 14-1 activity may have been measuring the consequences of ROS on cell viability/apoptotic fate, in lieu of or in addition to its effect of antagonizing antiapoptotic Bcl-2 family proteins. Synthesis of the more stable analog sHA 14-1 alleviated the decomposition problem, and generation of ROS was negligible (Tian et al., 2008). The goal of the current study was to elucidate the mechanism(s) underlying the proapoptotic activity of sHA 14-1.

Because antiapoptotic Bcl-2 family proteins can localize to the ER and regulate apoptosis through calcium homeostasis, small-molecule antagonists can potentially affect cellular calcium homeostasis. We found that sHA 14-1 rapidly induced an increase in cytosolic calcium through release of ER calcium storage in a dose-dependent manner (Fig. 2, A and B). We further demonstrated that sHA 14-1 induced the release of an ER calcium storage pool indistinguishable from the potent SERCA inhibitor thapsigargin, because addition of thapsigargin after sHA 14-1 treatment induced no further calcium release (Fig. 2, E and F). Although the intensity of calcium release induced by sHA 14-1 was not as pronounced as thapsigargin, the kinetics was similar (Fig. 2, C–F). The cytosolic calcium increase was at least partially responsible for the cytotoxicity of sHA 14-1, because its chelation resulted in protection of cells against sHA 14-1 (Fig. 3A). The partial protection through chelation is probably due to the incomplete suppression of cytosolic calcium increase. In addition, ER calcium depletion may function as a cytotoxic signal that can not be affected by cytosolic calcium chelation (Boelens et al., 2007).

The results in Figs. 2 and 3A did not clarify whether the cellular target of sHA 14-1 responsible for ER calcium release localized to the ER. However, disruption of mitochondrial function using FCCP, a mitochondria uncoupling agent, revealed that sHA 14-1 was still capable of reducing ER calcium storage in permeabilized NALM-6 and U937 leukemic cells (Fig. 3, B–D). These results suggest that at least one of the molecular targets of sHA 14-1 localizes to the ER.

Several transporters control ER calcium homeostasis, including IP_3Rs and SERCAs. Both have been reported to be regulated by Bcl-2 family proteins (Kuo et al., 1998; Li et al., 2002, 2007; Chen et al., 2004; Dremina et al., 2004, 2006; Oakes et al., 2005; White et al., 2005; Hanson et al., 2008). We used DT-40 and IP_3R-null DT-40 cells to determine the potential role of IP_3Rs in sHA 14-1–induced calcium release. The results in Fig. 4 showed that an absence of IP_3Rs did not alter the sensitivity of DT-40 cells to the cytotoxic effect of sHA 14-1 and sHA 14-1–induced ER calcium release. These results suggest that IP_3Rs are unlikely to be directly targeted by sHA 14-1.

Despite the fact that sHA 14-1 is an antagonist of Bcl-2 and Bcl-X_L with increased binding potency compared with HA 14-1 (Tian et al., 2008), we were surprised to discover that sHA 14-1 partially blocked thapsigargin-induced ER calcium release in a dose-dependent manner (Fig. 5, A and B). This result suggests that sHA 14-1 may induce ER calcium release through the SERCA pathway. This was confirmed by showing that sHA 14-1 inhibited the activity of both SERCA 1A and 2B (Fig. 5, C and D). Although Bcl-2 has been reported to regulate the function of SERCAs (Kuo et al., 1998; Dremina et al., 2004, 2006), our studies suggest that sHA 14-1 probably directly antagonizes SERCAs to induce ER calcium release, because no Bcl-2 protein was detected in the SERCA samples (Fig. 5E). The paradoxical capability of sHA 14-1 to suppress thapsigargin-induced ER calcium release (Fig. 5, A and B) probably exists because thapsigargin has a higher intrinsic activity to induce ER calcium release through SERCAs, whereas sHA 14-1 has a lower intrinsic activity. In addition to the effects on ER calcium and SERCA activity, sHA 14-1 treatment led to induction of ATF4 (Fig. 6). Thus, sHA 14-1 has a functional effect on the ER similar to thapsigargin, with a rapid release of ER calcium followed by subsequent ATF4 induction.

sHA 14-1 induced a loss of $\Delta\psi m$ (Fig. 7A) and caspase-9 activation (Fig. 6C) in leukemic cell lines 2 to 6 h after treatment. Its inactive counterpart, isHA 14-1, failed to induce a loss of $\Delta\psi m$ and caspase-9 activation under the same conditions, whereas ABT-737 induced a much more prominent loss of $\Delta\psi m$ (Fig. 7A) and caspase-9 activation (Fig. 6C). It remains to be determined whether there are ER/mitochondrial communications in response to sHA 14-1–induced stress or whether these are two independent processes.

The parent compound HA 14-1 has been reported to affect ER and mitochondrial function (An et al., 2004). However, those results might be attributable to the production of ROS after the rapid decomposition of HA 14-1 (Zhang et al., 2006; Doshi et al., 2007). In our own studies of HA 14-1, we noted effects on $\Delta\psi m$ and caspase-9 activation within 1 to 2 h after treatment (data not shown), whereas comparable effects by sHA 14-1 required 6 to 8 h (Fig. 7). The slower kinetics of cell death, the paucity of mitochondrial outer membrane permeabilization, the weak caspase-9 activation, and the relative insensitivity to the pan-caspase inhibitor *Z*-VAD-fmk are all consistent with a caspase-independent mechanism of cell death induced by sHA 14-1 (Tait and Green, 2008). The prominent change in the light scatter characteristics of

sHA 14-1 treated cells (Fig. 8) is suggestive of subcellular vacuole accumulation, and we are currently investigating whether this includes an autophagic component.

In conclusion, the current study shows that sHA 14-1, a small-molecule antagonist of antiapoptotic Bcl-2 family proteins, can exhibit subcellular targeting effects that encompass two vulnerable sites for initiation of apoptosis. Our collective data suggest a model wherein sHA 14-1 targets SERCAs in ER with a higher potency than the antiapoptotic Bcl-2 family proteins in the mitochondria. This model is supported by the rapid induction of ER calcium loss (Fig. 2) and the subsequent induction of ATF4 (Fig. 6). An effect on mitochondrial function is not detectable until 6 to 8 h after sHA 14-1 treatment (Fig. 7). The mechanism of the proapoptotic effect of sHA 14-1 is therefore distinct from ABT-737, which primarily initiates apoptosis by targeting the mitochondria, and thapsigargin, which acts specifically at the ER. The capacity of a small molecule such as sHA 14-1 to bind multiple intracellular targets may be an attractive strategy to overcome drug resistance that emerges as a consequence of multigene mutations (Frantz, 2005).

Acknowledgments

We thank Dr. Chi Li (University of Louisville) for providing the DT-40 B lymphoma cell line and IP_3R-null DT-40 cell line. We also thank Trinh Nguyen for technical assistance.

References

Adams JM and Cory S (2007) The Bcl-2 apoptotic switch in cancer development and therapy. *Oncogene* **26:**1324–1337.

An J, Chen Y, and Huang Z (2004) Critical upstream signals of cytochrome *c* release induced by a novel Bcl-2 inhibitor. *J Biol Chem* **279:**19133–19140.

An J, Chervin AS, Nie A, Ducoff HS, and Huang Z (2007) Overcoming the radioresistance of prostate cancer cells with a novel Bcl-2 inhibitor. *Oncogene* **26:**652–661.

Bilmen JG and Michelangeli F (2002) Inhibition of the type 1 inositol 1,4,5-trisphosphate receptor by 2-aminoethoxydiphenylborate. *Cell Signal* **14:**955–960.

Birmachu W, Nisswandt FL, and Thomas DD (1989) Conformational transitions in the calcium adenosinetriphosphatase studied by time-resolved fluorescence resonance energy transfer. *Biochemistry* **28:**3940–3947.

Boelens J, Lust S, Offner F, Bracke ME, and Vanhoecke BW (2007) Review. The endoplasmic reticulum: a target for new anticancer drugs. *In Vivo* **21:**215–226.

Bollig A, Xu L, Thakur A, Wu J, Kuo TH, and Liao JD (2007) Regulation of intracellular calcium release and PP1alpha in a mechanism for 4-hydroxytamoxifen-induced cytotoxicity. *Mol Cell Biochem* **305:**45–54.

Breckenridge DG, Germain M, Mathai JP, Nguyen M, and Shore GC (2003) Regulation of apoptosis by endoplasmic reticulum pathways. *Oncogene* **22:**8608–8618.

Chen R, Valencia I, Zhong F, McColl KS, Roderick HL, Bootman MD, Berridge MJ, Conway SJ, Holmes AB, Mignery GA, et al. (2004) Bcl-2 functionally interacts with inositol 1,4,5-trisphosphate receptors to regulate calcium release from the ER in response to inositol 1,4,5-trisphosphate. *J Cell Biol* **166:**193–203.

Dai Y, Rahmani M, Corey SJ, Dent P, and Grant S (2004) A Bcr/Abl-independent, Lyn-dependent form of imatinib mesylate (STI-571) resistance is associated with altered expression of Bcl-2. *J Biol Chem* **279:**34227–34239.

Del Gaizo Moore V, Schlis KD, Sallan SE, Armstrong SA, and Letai A (2008) BCL-2 dependence and ABT-737 sensitivity in acute lymphoblastic leukemia. *Blood* **111:** 2300–2309.

Denmeade SR and Isaacs JT (2005) The SERCA pump as a therapeutic target: making a "smart bomb" for prostate cancer. *Cancer Biol Ther* **4:**14–22.

Doshi JM, Tian D, and Xing C (2007) Ethyl-2-amino-6-bromo-4-(1-cyano-2-ethoxy-2-oxoethyl)-4*H*- chromene-3-carboxylate (HA 14-1), a prototype small-molecule antagonist against antiapoptotic Bcl-2 proteins, decomposes to generate reactive oxygen species that induce apoptosis. *Mol Pharm* **4:**919–928.

Doshi JM and Xing C (2008) Antagonists against anti-apoptotic Bcl-2 family proteins for cancer treatment. *Mini Rev Org Chem* **5:**171–178.

Dremina ES, Sharov VS, Kumar K, Zaidi A, Michaelis EK, and Schöneich C (2004) Anti-apoptotic protein Bcl-2 interacts with and destabilizes the sarcoplasmic/endoplasmic reticulum Ca^{2+}-ATPase (SERCA). *Biochem J* **383:**361–370.

Dremina ES, Sharov VS, and Schöneich C (2006) Displacement of SERCA from SR lipid caveolae-related domains by Bcl-2: a possible mechanism for SERCA inactivation. *Biochemistry* **45:**175–184.

Fernandez JL, Rosemblatt M, and Hidalgo C (1980) Highly purified sarcoplasmic reticulum vesicles are devoid of Ca^{2+}-independent ('basal') ATPase activity. *Biochim Biophys Acta* **599:**552–568.

Frantz S (2005) Drug discovery: playing dirty. *Nature* **437**:942–943.

Giorgi C, Romagnoli A, Pinton P, and Rizzuto R (2008) Ca^{2+} signaling, mitochondria and cell death. *Curr Mol Med* **8**:119–130.

Hanson CJ, Bootman MD, Distelhorst CW, Wojcikiewicz RJ, and Roderick HL (2008) Bcl-2 suppresses Ca^{2+} release through inositol 1,4,5-trisphosphate receptors and inhibits Ca^{2+} uptake by mitochondria without affecting ER calcium store content. *Cell Calcium* **44:**324–338.

Hurwitz R, Hozier J, LeBien T, Minowada J, Gajl-Peczalska K, Kubonishi I, and Kersey J (1979) Characterization of a leukemic cell line of the pre-B phenotype. *Int J Cancer* **23:**174–180.

Hutson SM, Pfeiffer DR, and Lardy HA (1976) Effect of cations and anions on the steady state kinetics of energy-dependent Ca^{2+} transport in rat liver mitochondria. *J Biol Chem* **251:**5251–5258.

Krajewski S, Tanaka S, Takayama S, Schibler MJ, Fenton W, and Reed JC (1993) Investigation of the subcellular distribution of the bcl-2 oncoprotein: residence in the nuclear envelope, endoplasmic reticulum, and outer mitochondrial membranes. *Cancer Res* **53:**4701–4714.

Kuo TH, Kim HR, Zhu L, Yu Y, Lin HM, and Tsang W (1998) Modulation of endoplasmic reticulum calcium pump by Bcl-2. *Oncogene* **17:**1903–1910.

Lee DI, Sumbilla C, Lee M, Natesavelalar C, Klein MG, Ross DD, Inesi G, and Hussain A (2007) Mechanisms of resistance and adaptation to thapsigargin in androgen-independent prostate cancer PC3 and DU145 cells. *Arch Biochem Biophys* **464:**19–27.

Letai A (2005) Pharmacological manipulation of Bcl-2 family members to control cell death. *J Clin Invest* **115:**2648–2655.

Letai AG (2008) Diagnosing and exploiting cancer's addiction to blocks in apoptosis. *Nat Rev Cancer* **8:**121–132.

Li C, Fox CJ, Master SR, Bindokas VP, Chodosh LA, and Thompson CB (2002) Bcl-X(L) affects Ca^{2+} homeostasis by altering expression of inositol 1,4,5-trisphosphate receptors. *Proc Natl Acad Sci U S A* **99:**9830–9835.

Li C, Wang X, Vais H, Thompson CB, Foskett JK, and White C (2007) Apoptosis regulation by Bcl-x(L) modulation of mammalian inositol 1,4,5-trisphosphate receptor channel isoform gating. *Proc Natl Acad Sci U S A* **104:**12565–12570.

Lickliter JD, Cox J, McCarron J, Martinez NR, Schmidt CW, Lin H, Nieda M, and Nicol AJ (2007) Small-molecule Bcl-2 inhibitors sensitise tumour cells to immune-mediated destruction. *Br J Cancer* **96:**600–608.

Lickliter JD, Wood NJ, Johnson L, McHugh G, Tan J, Wood F, Cox J, and Wickham NW (2003) HA14-1 selectively induces apoptosis in Bcl-2-overexpressing leukemia/lymphoma cells, and enhances cytarabine-induced cell death. *Leukemia* **17:**2074–2080.

Liu X, Lee K, and Herbison AE (2008) Kisspeptin excites gonadotropin-releasing hormone neurons through a phospholipase C/calcium-dependent pathway regulating multiple ion channels. *Endocrinology* **149:**4605–4614.

Manero F, Gautier F, Gallenne T, Cauquil N, Grée D, Cartron PF, Geneste O, Grée R, Vallette FM, and Juin P (2006) The small organic compound HA14-1 prevents Bcl-2 interaction with Bax to sensitize malignant glioma cells to induction of cell death. *Cancer Res* **66:**2757–2764.

Michelangeli F and Munkonge FM (1991) Methods of reconstitution of the purified sarcoplasmic reticulum (Ca^{2+}-Mg^{2+})-ATPase using bile salt detergents to form membranes of defined lipid to protein ratios or sealed vesicles. *Anal Biochem* **194:**231–236.

Milella M, Estrov Z, Kornblau SM, Carter BZ, Konopleva M, Tari A, Schober WD, Harris D, Leysath CE, Lopez-Berestein G, et al. (2002) Synergistic induction of apoptosis by simultaneous disruption of the Bcl-2 and MEK/MAPK pathways in acute myelogenous leukemia. *Blood* **99:**3461–3464.

Milella M, Trisciuoglio D, Bruno T, Ciuffreda L, Mottolese M, Cianciulli A, Cognetti F, Zangemeister-Wittke U, Del Bufalo D, and Zupi G (2004) Trastuzumab down-regulates Bcl-2 expression and potentiates apoptosis induction by Bcl-2/Bcl-XL bispecific antisense oligonucleotides in HER-2 gene-amplified breast cancer cells. *Clin Cancer Res* **10:**7747–7756.

Niizuma H, Nakamura Y, Ozaki T, Nakanishi H, Ohira M, Isogai E, Kageyama H, Imaizumi M, and Nakagawara A (2006) Bcl-2 is a key regulator for the retinoic acid-induced apoptotic cell death in neuroblastoma. *Oncogene* **25:**5046–5055.

Nimmanapalli R, O'Bryan E, Kuhn D, Yamaguchi H, Wang HG, and Bhalla KN (2003) Regulation of 17-AAG-induced apoptosis: role of Bcl-2, Bcl-XL, and Bax downstream of 17-AAG-mediated down-regulation of Akt, Raf-1, and Src kinases. *Blood* **102:**269–275.

O'Neill JP, Velalar CN, Lee DI, Zhang B, Nakanishi T, Tang Y, Selaru F, Ross D, Meltzer SJ, and Hussain A (2006) Thapsigargin resistance in human prostate cancer cells. *Cancer* **107:**649–659.

Oakes SA, Scorrano L, Opferman JT, Bassik MC, Nishino M, Pozzan T, and Korsmeyer SJ (2005) Proapoptotic BAX and BAK regulate the type 1 inositol trisphosphate receptor and calcium leak from the endoplasmic reticulum. *Proc Natl Acad Sci* **102:**105–110.

Oltersdorf T, Elmore SW, Shoemaker AR, Armstrong RC, Augeri DJ, Belli BA, Bruncko M, Deckwerth TL, Dinges J, Hajduk PJ, et al. (2005) An inhibitor of Bcl-2 family proteins induces regression of solid tumours. *Nature* **435**:677–681.

Ow YP, Green DR, Hao Z, and Mak TW (2008) Cytochrome c: functions beyond respiration. *Nat Rev Mol Cell Biol* **9:**532–542.

Pei XY, Dai Y, and Grant S (2003) The proteasome inhibitor bortezomib promotes mitochondrial injury and apoptosis induced by the small molecule Bcl-2 inhibitor HA14-1 in multiple myeloma cells. *Leukemia* **17:**2036–2045.

Pei XY, Dai Y, and Grant S (2004) The small-molecule Bcl-2 inhibitor HA14-1 interacts synergistically with flavopiridol to induce mitochondrial injury and apoptosis in human myeloma cells through a free radical-dependent and Jun NH2-terminal kinase-dependent mechanism. *Mol Cancer Ther* **3:**1513–1524.

Pinton P, Ferrari D, Rapizzi E, Di Virgilio F, Pozzan T, and Rizzuto R (2001) The Ca^{2+} concentration of the endoplasmic reticulum is a key determinant of ceramide-induced apoptosis: significance for the molecular mechanism of Bcl-2 action. *EMBO J* **20:**2690–2701.

Pinton P and Rizzuto R (2006) Bcl-2 and Ca^{2+} homeostasis in the endoplasmic reticulum. *Cell Death Differ* **13:**1409–1418.

Reddy LG, Cornea RL, Winters DL, McKenna E, and Thomas DD (2003) Defining the molecular components of calcium transport regulation in a reconstituted membrane system. *Biochemistry* **42:**4585–4592.

Reed JC (2003) Apoptosis-targeted therapies for cancer. *Cancer Cell* **3:**17–22.
Reed JC (2008) Bcl-2-family proteins and hematologic malignancies: history and future prospects. *Blood* **111:**3322–3330.
Rong Y and Distelhorst CW (2008) Bcl-2 protein family members: versatile regulators of calcium signaling in cell survival and apoptosis. *Annu Rev Physiol* **70:**73–91.
Scorrano L, Oakes SA, Opferman JT, Cheng EH, Sorcinelli MD, Pozzan T, and Korsmeyer SJ (2003) BAX and BAK regulation of endoplasmic reticulum Ca^{2+}: a control point for apoptosis. *Science* **300:**135–139.
Shah N, Asch RJ, Lysholm AS, and Lebien TW (2004) Enhancement of stress-induced apoptosis in B-lineage cells by caspase-9 inhibitor. *Blood* **104:**2873–2878.
Sinicrope FA, Penington RC, and Tang XM (2004) Tumor necrosis factor-related apoptosis-inducing ligand-induced apoptosis is inhibited by Bcl-2 but restored by the small molecule Bcl-2 inhibitor, HA 14-1, in human colon cancer cells. *Clin Cancer Res* **10:**8284–8292.
Sinicrope FA and Penington RC (2005) Sulindac sulfide-induced apoptosis is enhanced by a small-molecule Bcl-2 inhibitor and by TRAIL in human colon cancer cells overexpressing Bcl-2. *Mol Cancer Ther* **4:**1475–1483.
Stong RC, Korsmeyer SJ, Parkin JL, Arthur DC, and Kersey JH (1985) Human acute leukemia cell line with the t(4;11) chromosomal rearrangement exhibits B lineage and monocytic characteristics. *Blood* **65:**21–31.
Sugawara H, Kurosaki M, Takata M, and Kurosaki T (1997) Genetic evidence for involvement of type 1, type 2 and type 3 inositol 1,4,5-trisphosphate receptors in signal transduction through the B-cell antigen receptor. *EMBO J* **16:**3078–3088.
Szalai G, Krishnamurthy R, and Hajnóczky G (1999) Apoptosis driven by IP(3)-linked mitochondrial calcium signals. *EMBO J* **18:**6349–6361.
Tait SW and Green DR (2008) Caspase-independent cell death: leaving the set without the final cut. *Oncogene* **27:**6452–6461.
Thomenius MJ and Distelhorst CW (2003) Bcl-2 on the endoplasmic reticulum: protecting the mitochondria from a distance. *J Cell Sci* **116:**4493–4499.
Tian D, Das SG, Doshi JM, Peng J, Lin J, and Xing C (2008) sHA 14-1, a stable and ROS-free antagonist against anti-apoptotic Bcl-2 proteins, bypasses drug resistances and synergizes cancer therapies in human leukemia cell. *Cancer Lett* **259:**198–208.
Wang JL, Liu D, Zhang ZJ, Shan S, Han X, Srinivasula SM, Croce CM, Alnemri ES, and Huang Zuang Z (2000) Structure-based discovery of an organic compound that binds Bcl-2 protein and induces apoptosis of tumor cells. *Proc Natl Acad Sci U S A* **97:**7124–7129.
White C, Li C, Yang J, Petrenko NB, Madesh M, Thompson CB, and Foskett JK (2005) The endoplasmic reticulum gateway to apoptosis by Bcl-X(L) modulation of the InsP3R. *Nat Cell Biol* **7:**1021–1028.
Wootton LL and Michelangeli F (2006) The effects of the phenylalanine 256 to valine mutation on the sensitivity of sarcoplasmic/endoplasmic reticulum Ca^{2+} ATPase (SERCA) Ca^{2+} pump isoforms 1, 2, and 3 to thapsigargin and other inhibitors. *J Biol Chem* **281:**6970–6976.
Wörmann B, Anderson JM, Liberty JA, Gajl-Peczalska K, Brunning RD, Silberman TL, Arthur DC, and LeBien TW (1989) Establishment of a leukemic cell model for studying human pre-B to B cell differentiation. *J Immunol* **142:**110–117.
Xu C, Bailly-Maitre B, and Reed JC (2005) Endoplasmic reticulum stress: cell life and death decisions. *J Clin Invest* **115:**2656–2664.
Zhang Y, Soboloff J, Zhu Z, and Berger SA (2006) Inhibition of Ca^{2+} influx is required for mitochondrial reactive oxygen species-induced endoplasmic reticulum Ca^{2+} depletion and cell death in leukemia cells. *Mol Pharmacol* **70:**1424–1434.
Zong WX, Li C, Hatzivassiliou G, Lindsten T, Yu QC, Yuan J, and Thompson CB (2003) Bax and Bak can localize to the endoplasmic reticulum to initiate apoptosis. *J Cell Biol* **162:**59–69.

Address correspondence to: Dr. Chengguo Xing, 308 Harvard St. SE, Minneapolis, MN 55455. E-mail: xingx009@umn.edu